PHYSICAL REVIEW B **88**, 081402(R) (2013)

Anomalous thermal expansion of γ-iron nanocrystals inside multiwalled carbon nanotubes

Julien Cambedouzou,[1,2,*] Périne Landois,[1,3,4] Stéphan Rouzière,[1] Mathieu Pinault,[3] Cristian Mocuta,[5] Louis Hennet,[6] Dominique Thiaudière,[5] Martine Mayne-L'Hermite,[3] and Pascale Launois[1]

[1]*Laboratoire de Physique des Solides, UMR CNRS 8502, Université Paris Sud, F-91405 Orsay, France*

[2]*Institut de Chimie Séparative de Marcoule, UMR 5257 CEA/CNRS/UM2/ENSCM, F-30207 Bagnols sur Cèze, France*

[3]*CEA-IRAMIS-SPAM, Laboratoire Francis Perrin (CNRS URA 2453), 91191 Gif-sur-Yvette, France*

[4]*Laboratoire Charles Coulomb UMR 5221 CNRS/Université Montpellier 2, F-34095 Montpellier, France*

[5]*Synchrotron Soleil, Saint Aubin BP 48, 91191 Gif-sur-Yvette, France*

[6]*CEMHTI-CNRS UPR3079, F-45071 Orléans Cedex 2, France*

(Received 29 May 2013; published 8 August 2013)

The thermal expansion of α-Fe (ferrite) and γ-Fe (austenite) nanocrystals confined inside multiwalled carbon nanotubes (MWCNTs) is studied *in situ*, using synchrotron x-ray diffraction, as a function of temperature. While the thermal expansion of ferrite is similar to that of bulk material, a peculiar behavior is evidenced for austenite: The thermal expansion becomes abnormally high above 500 °C. A scenario involving progressive carbon uptake in γ-Fe nanocrystals gives a satisfactory understanding of the phenomenon, and allows one to propose a value of the carbon solubilization rate in γ-Fe particles confined inside MWCNTs.

DOI: 10.1103/PhysRevB.88.081402 PACS number(s): 61.05.cp, 61.46.−w, 65.40.De

I. INTRODUCTION

Important advances have been realized concerning the understanding of the growth mechanisms and the physical properties of carbon nanotubes (CNTs) since their discovery more than 20 years ago. Thanks to the development of chemical vapor deposition (CVD) synthesis methods, better control of the physical parameters of CNTs, in terms of the number of walls and overall dimensions, is now possible. Technological bottlenecks are progressively overcome and applications of CNTs are under development in various fields,[1] such as interconnects,[2] membranes for separation or filtering,[3] composites for aerospace applications,[4] or sensors.[5] In parallel to the fascinating applications CNTs are dedicated for, these objects offer the opportunity to study confined systems. They can indeed be viewed as nanometer sized containers in which matter can be confined, and where physics and chemistry are different from the ones in the usual three-dimensional case. Examples are too numerous to be all quoted. The reader could, for example, refer to review articles on water,[6] fullerenes,[7] and other molecules and crystals[8] in nanotubes. In the case of aerosol-assisted catalytic CVD (CCVD) consisting of a continuous feeding of the reactor with both the metal catalytic source and the hydrocarbon source, CCVD synthesis of multiwalled carbon nanotube (MWCNT) carpets is accompanied by the production of iron-based nanometer sized crystals inside the MWCNT. In the early stages, the thermal decomposition of the metal catalytic source involves the nucleation of the catalytic particles[9] from which MWCNTs grow, following a base growth mechanism.[10] Then, these catalytic particles are continuously fed with metal species, resulting in a particle growth and a subsequent detachment of part of the particle inside the MWCNT, when it grows.[11] These particles can be found under the form of γ-Fe, which is not the stable phase of iron under ambient temperature and pressure conditions. The existence of γ-Fe is frequently attributed to the confinement of iron nanocrystals in the tube.[12,13] In this Rapid Communication, we report on the anomalous thermal expansion behavior we observed for confined iron-based nanoparticles. A surprisingly large thermal expansion was observed in confined γ-Fe for temperatures above 500 °C, while it can be considered as normal when the temperature is lower. We discuss possible explanations for this anomaly and propose a hypothesis of reversible carbon uptake and loss in the atomic structure of iron particles. We give a quantification of the thermal rate of this phenomenon.

II. MATERIALS AND METHODS

Vertically aligned MWCNT (VA-MWCNT) carpets are synthesized by aerosol-assisted CCVD (AA-CCVD) from toluene and ferrocene (2.5 wt % ferrocene dissolved in toluene) precursors. This precursor mixture is injected continuously through an aerosol and carried by a helium flow (1.5 l/min) at 850 °C. Thin silicon wafers (10 μm) are placed in the center of the furnace. The duration of the AA-CCVD process is 15 min, allowing to obtain a VA-MWCNT of 600 μm length [length measured by scanning electron microscopy in a field emission gun scanning electron microscope (FEG-SEM) Carl Zeiss Ultra 55]. From high resolution transmission electron microscopy (HRTEM) performed with a Philips CM 20 operating at 200 kV, iron-based particles can be clearly identified mainly in the inner core of the MWCNT and are typically less than 10 nm large and up to 100 nm long [see Fig. 1(a) and the Supplemental Material].[14] Temperature dependent *in situ* x-ray diffraction measurements were performed on the Diffabs beamline at the SOLEIL synchrotron.[15] The x-ray energy was set to 17.035 keV, corresponding to a wavelength of 0.7279 Å. Si wafers were pasted on alumina holders using refractory cement withstanding the high temperature thermal treatments (1200 °C) that were applied to our samples. These holders were mounted in a Buhler x-ray powder diffraction oven[16] under secondary vacuum, allowing temperatures as high as 1500 °C to be reached. A 180° arc-shaped window on the curved face of the cylindrical oven chamber allows both the incident beam to enter the oven and the diffracted beams to exit it [see Fig. 1(b)]. This window is made of

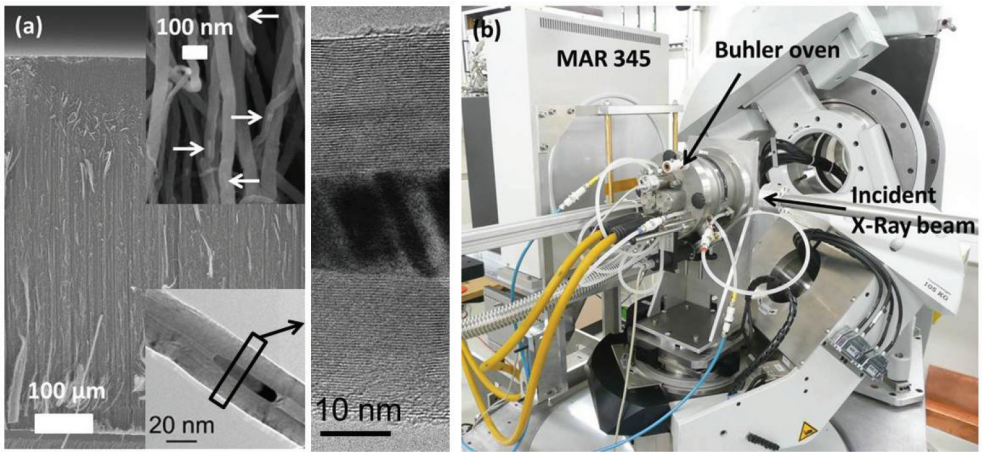

FIG. 1. (Color online) (a) SEM image of a VA-MWCNT carpet. Insets: Magnification of the SEM image (top) and TEM image of an iron-based nanoparticle inside the MWCNT inner core (bottom) with HRTEM magnification of the image exhibiting the encapsulation of the nanoparticle into the central core of the MWCNT. Arrows in the SEM magnification point toward iron-based particles, which appear as bright objects in the MWCNT inner core. (b) Photograph of the experimental setup mounted on the Diffabs beamline at SOLEIL synchrotron, with a Buhler oven and a MAR 345 detector.

varnish-coated beryllium, and the corresponding diffraction signal was carefully identified in order to separate it from the signal coming from the sample. The MWCNT carpets were placed in such a way that the axis of the MWCNT was parallel to the incident beam. Diffraction patterns were recorded with a MAR 345 imaging plate detector, placed behind the sample (i.e., the setup is in transmission geometry). Intensity versus scattering vector Q curves were obtained by radial integration of the signal over the part of the imaging plate facing the exit window of the oven. Acquisition durations of 2 and 10 s were alternatively used, in order to obtain an optimal signal-to-noise ratio for the signal coming from the graphitic stacking of MWCNT walls (intense signal, 2 s acquisitions) and from iron-based phases (less intense signals, 10 s acquisitions), respectively. Typical temperature ramping rates were of 5 °C per minute.

III. RESULTS AND DISCUSSION

CCVD grown carpets of VA-MWCNT contain different iron-based crystals of nanometer size.[17] X-ray diffraction (XRD) is a valuable tool to identify these phases, and to further study their structural characteristics. Figure 2 shows the XRD diagram of the MWCNT carpet at 50 °C. The complete indexation of the diffraction peaks appearing in this diagram can be found elsewhere.[17] We only reported in the figure the Miller indices of the peaks that are studied in this work.

The most intense peak, observed at a scattering vector Q of 18.3 nm^{-1}, is attributed to MWCNT. It corresponds to a mean distance of ∼0.34 nm between concentric graphene sheets of MWCNT. Such a distance is similar to that found in graphite. This peak is further referred to as "C 002." A large number of other peaks are visible, though their intensity is much smaller. The magnification presented in Fig. 2 allows to identify all present phases. Iron-based nanoparticles are iron oxide Fe_3O_4, iron carbide Fe_3C, body-centered-cubic ferrite α-Fe, and face-centered-cubic (fcc) austenite γ-Fe, as already discussed in Ref. 16 and in other studies involving Mössbauer spectroscopy.[18,19] In particular, γ-Fe is not expected to exist as a stable phase at 50 °C and should have transformed into α-Fe during the cooling step after the synthesis. However, this transformation requires a huge *radial* expansion (12%) of the lattice parameter in two directions, which may be hindered by the lateral confinement exerted by the tube, explaining the persistence of γ-Fe down to low temperature.[12,13] The compressibility and the thermal expansion of materials are related to their structure and to the nature of the interactions between their constituting atoms. In a previous article, we studied the compressibility of the different phases that can be found in MWCNTs through *in situ* high pressure synchrotron XRD measurements.[20] We found that the compressibility of MWCNT walls was similar to that of graphite, which is in line with the structural hypothesis of a defective Russian doll-like structure,[21] i.e., where concentric layers contain defects that lower the stress inherent in the Russian doll structure. The left part of Fig. 3 presents the relative thermal expansion of the

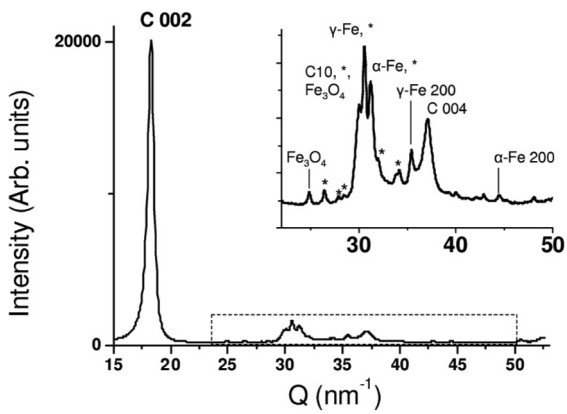

FIG. 2. XRD diagram of the MWCNT sample at $T = 50$ °C. The MWCNT peaks are denoted as C 00l ($l = 2, 4$) and C10. The inset is a magnification of the intensity in the 22–50 nm^{-1} range. The identification of the main peaks is given, and asterisks (∗) indicate Fe_3C peaks.

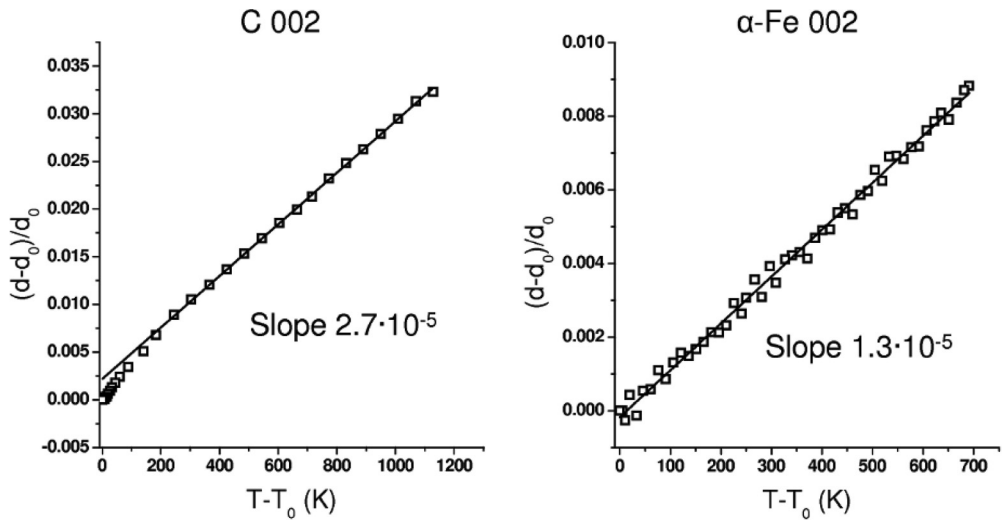

FIG. 3. Thermal expansion of the C 002 distance in the MWCNT (left) and of the 002 inter-reticular distance in ferrite (right). Experimental points appear as squares and lines are linear fits (slopes are provided).

interwall distance of MWCNT (deduced from the C 002 peak position, as a function of temperature). The thermal expansion coefficient referred to as A in this Rapid Communication is defined as

$$\frac{d - d_0}{d_0} = A\,(T - T_0)\,, \tag{1}$$

where $d = 2\pi/Q$ is the reticular distance at temperature T and d_0 is the reference reticular distance at temperature T_0 ($T_0 = 50\,^{\circ}$C in our case).

The thermal expansion of the C 002 interwall distance is found to be $A_{C002} = 2.7 \times 10^{-5}$ K^{-1}. This value is close to that of graphite, which is of 2.8×10^{-5} K^{-1},[22] as already stated in other studies.[23,24] The good agreement between our results and those from the literature is positive confirmation of the reliability of our measurements.

We now focus on the thermal behavior of the iron-based phases contained in our VA-MWCNT sample. Note that the Bragg peaks related to Fe_3C nanoparticles are of low intensity and in the vicinity of more intense Bragg peaks related to other nanocrystals. The thermal expansion of Fe_3C nanoparticles is therefore very difficult to follow and will not be discussed here. The right part of Fig. 3 shows the thermal expansion of the 200 distance in α-Fe ferrite. The lattice parameter of ferrite varies linearly with temperature. The thermal expansion is found to be of 1.3×10^{-5} K^{-1}. This value is in very good agreement with that given in the literature for bulk ferrite, which is around 1.4×10^{-5} K^{-1}.[25] This result suggests that the confinement of α-Fe inside a MWCNT has no measurable influence on its thermal expansion. The thermal behavior of the 002 reticular distance of fcc γ-Fe is reported in Fig. 4, for both the temperature increase and decrease.

The thermal behavior of γ-Fe nanocrystals is clearly different from that of α-Fe. A clear change in the thermal expansion slope is observed during both heating and cooling. It occurs at temperatures between 400 and 500 °C. Below 400 °C, the thermal expansion is equal to 2.0×10^{-5} K^{-1}, and above 500 °C it is equal to 3.7×10^{-5} K^{-1}. We report here a determination of the thermal expansion of γ-Fe confined inside a CNT, and, because similar determinations are lacking, a comparison could not be made to values from the literature. An interesting comparison can, however, be made with the thermal expansion of γ-Fe nanoinclusions in FeCu crystals.[26] In such materials, γ-Fe nanocrystals can be found down to ambient temperature. The thermal expansion was reported to be $A = 2.2 \times 10^{-5}$ K^{-1} in the latter material, i.e., close to the value we measure in the lower temperature range (2.0×10^{-5} K^{-1}). Contrarily to our results, no change was observed in the thermal expansion at higher temperatures.

A thermal expansion of 3.7×10^{-5} K^{-1} is very large, and quite unusual for iron. A major difference between γ-Fe nanoinclusions in FeCu crystals and γ-Fe nanoparticles in MWCNTs is their chemical environment. We propose that the increased thermal expansion we observe could originate from the gradual intercalation of carbon atoms in the fcc lattice of γ-Fe as interstitial atoms. Such a phenomenon is likely, considering the large amount of carbon available in the vicinity

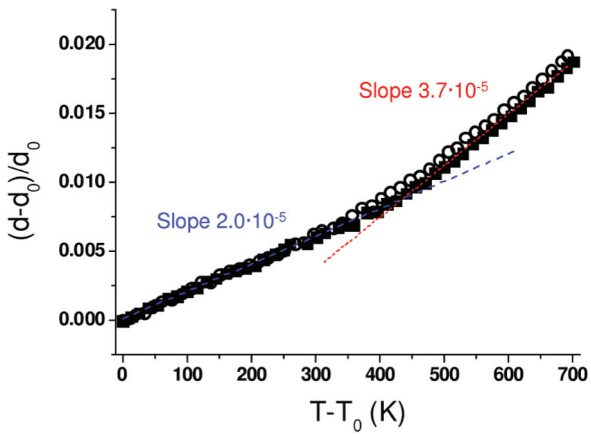

FIG. 4. (Color online) Thermal expansion of the 200 inter-reticular distance of γ-Fe. Squares and circles represent experimental points obtained during the temperature increase and decrease, respectively. Lines represent linear fits of the data and the corresponding slopes are given.

of iron-based particles. The diffusion of carbon atoms from CNTs toward catalytic particles was observed under electron irradiation in a transmission electron microscope.[27] The insertion of carbon atoms into γ-Fe particles, at high temperature in our study, would result in an increase of the lattice parameter of the γ-Fe crystal cumulating with the thermal expansion.

The intercalation of carbon atoms in γ-Fe was studied by Onink *et al.* in 1993.[28] Two interesting results emerged from this study. First, carbon atom intercalation into γ-Fe results in the expansion of its lattice parameter, following a slope estimated at 7.0×10^{-4} nm per carbon atom inserted in 100 Fe atoms (Fig. 4 in Ref. 28). Second, the insertion of carbon atoms into γ-Fe causes a very small decrease of the thermal expansion of γ-Fe. Figure 5 in Ref. 28 indeed shows that thermal expansion is lowered by -0.05×10^{-5} K^{-1} per inserted C atom in 100 Fe atoms. Considering that the thermal expansion of γ-Fe is equal to 2.0×10^{-5} K^{-1} for temperatures lower than 500 °C (Fig. 4), it will not be significantly modified by the insertion of a few C atoms per 100 Fe atoms. Consequently, in the following, the increase of the expansion coefficient above 500 °C is considered as essentially due to a progressive uptake of carbon atoms, depending on the temperature.

In order to measure the single effect of carbon intercalation on the expansion of the γ-Fe lattice parameter, we subtracted the thermal expansion measured at lower temperatures from the one measured at higher temperatures. The excess of lattice expansion observed when $T > 500$ °C is $(3.7-2.0) \times 10^{-5} = 1.7 \times 10^{-5}$ K^{-1}. We attribute it to carbon intercalation into the austenitic structure. We can describe this lattice expansion by the following equation, which is only valid for $T > T_C = 500$ °C:

$$\frac{d - d_C}{d_C} = 1.7 \times 10^{-5} (T - T_C), \tag{2}$$

where d_C is the reticular distance at temperature T_C. Defining ΔX_C as the number of additional carbon atoms for 100 iron atoms, we have, on the other hand,

$$a = a_C + 7.0 \times 10^{-4} \Delta X_C, \tag{3}$$

where a_C is the lattice parameter (in nm) of γ-Fe at temperature T_C. In a cubic system, d is proportional to a, and combining (2) and (3) gives

$$\Delta X_C = 2.4 \times 10^{-2} a_C (T - T_C). \tag{4}$$

Considering that $a_C = 2(2\pi / Q_{200}) = 0.3582$ nm ($Q_{002} = 35.079$ nm^{-1} at T_C, according to experimental data), we obtain $\Delta X_C = 2.1$ at a temperature of 750 °C, meaning that the solubilization of carbon reaches 2.1 at./100 Fe atoms. Note that the purely thermal expansion is expected to be decreased by less than 3% for such a carbon uptake, which validates our approximation of unchanged thermal expansion. We therefore determined a carbon thermal solubilization rate of 8.4×10^{-3} Carbon at. K^{-1} for confined γ-Fe particles when the temperature is higher than 500 °C. It is interesting to note that the same slope change in the variation of parameter with temperature appears both during the temperature increase and decrease (Fig. 4). The phenomenon of carbon uptake is thus reversible.

A simple calculation, considering a nanoparticle lateral size of 10 nm, shows that a carbon uptake of 2.1 at./100 Fe atoms corresponds to the incorporation of ~140 carbon atoms per 1 nm height in the Fe nanoparticle. It is interesting to compare this value to the total number of C atoms in the inner shell of the MWCNT, of ~1160 atom per 1 nm in height for an internal tube diameter of 10 nm (the atomic surface density of graphene is 37 atoms/nm^2). The internal graphene sheet of the MWCNT is thus a sufficient reservoir in carbon to explain the carbon uptake in γ-Fe. Finally, let us discuss why no anomalous thermal expansion was observed for α-Fe, while those nanoparticles are also surrounded by the nanotube. We attribute it to the fact that the α-Fe phase in its bulk phase is known to accept only a very small quantity of carbon. This small uptake ability can be seen in the Fe-C phase diagram, where the existence domain of the α-Fe phase is restricted to carbon contents lower than 0.02 wt %.

IV. CONCLUSIONS

In conclusion, we studied the thermal behavior of MWCNTs containing iron-based nanoparticles. The thermal expansion of the interlayer distance of MWCNTs was found similar to that of graphite, in good agreement with the literature. Concerning iron-based particles, α-Fe particles showed a thermal expansion identical to that of bulk iron, while we observed an anomalous thermal expansion of γ-Fe nanoparticles confined inside MWCNTs. For the latter nanoparticles, an increase of the variation of the 200 inter-reticular distance versus temperature was observed for temperatures larger than 500 °C. We propose that the excess thermal expansion is in fact due to the progressive solubilization of C into the γ-Fe fcc structure. These additional carbon atoms are probably taken from the vicinity of γ-Fe particles, and are reversibly going out from γ-Fe particles upon cooling. Based on previous experiments by Onink *et al.*,[27] we derive a thermal solubilization rate of 8.4×10^{-3} Carbon at. K^{-1} in γ-Fe nanocrystals. The possibility of tuning the interstitial carbon atom contents in the crystalline lattice of γ-Fe nanoparticles could open interesting perspectives for some applications, in particular, in the field of magnetism.[29]

ACKNOWLEDGMENTS

The authors thank J. N. Rouzaud (Laboratoire de Géologie, ENS, Paris) for HRTEM analyses, the CEA-DSV Saclay (TEM Team platform) for TEM observation facilities, the Région Ile de France for financial support for the SEM equipment, and the P-Nano program of the French Agence Nationale de la Recherche for its financial support on the "ALUCINAN" project.

*Corresponding author: julien.cambedouzou@enscm.fr

[1] M. F. L. De Volder, S. H. Tawfick, R. H. Baughman, and A. J. Hart, Science **339**, 535 (2013).

[2] S. Esconjauregui, M. Fouquet, B. C. Bayer, C. Ducati, R. Smajda, S. Hofmann, and J. Robertson, ACS Nano **4**, 7431 (2010).

[3]B. J. Hinds, N. Chopra, T. Rantell, R. Andrews, V. Gavalas, and L. G. Bachas, Science **303**, 62 (2004).
[4]B. L. Wardle, D. S. Saito, E. J. García, A. J. Hart, R. G. de Villoria, and E. A. Verploegen, Adv. Mater. **20**, 2707 (2008).
[5]C. Wei, L. Dai, A. Roy, and T. B. Tolle, J. Am. Chem. Soc. **128**, 1412 (2009).
[6]A. Noy, H. G. Park, F. Fornasiero, J. K. Holt, C. P. Grigoropoulos, and O. Bakajin, Nano Today **2**, 22 (2007).
[7]A. N. Khlobystov, D. A. Britz, and G. A. D. Briggs, Acc. Chem. Res. **38**, 901 (2005).
[8]M. Monthioux, E. Flahaut, and J. P. Cleuziou, J. Mater. Res. **21**, 2774 (2006).
[9]C. Castro, M. Pinault, S. Coste-Leconte, D. Porterat, N. Bendiab, C. Reynaud, and M. Mayne-L'Hermite, Carbon **48**, 3807 (2010).
[10]M. Pinault, V. Pichot, H. Khodja, P. Launois, C. Reynaud, and M. Mayne-L'Hermite, Nano Lett. **5**, 2394 (2005).
[11]R. Xiang, G. Luo, W. Qian, Q. Zhang, Y. Wang, F. Wei, Q. Li, and A. Cao, Adv. Mater. **19**, 2360 (2007).
[12]H. Kim, M. J. Haufman, W. M. Sigmund, D. Jacques, and R. Andrews, J. Mater. Res. **18**, 1104 (2003).
[13]V. Pichot, P. Launois, M. Pinault, M. Mayne-L'Hermite, and C. Reynaud, Appl. Phys. Lett. **85**, 473 (2004).
[14]See Supplemental Material at http://link.aps.org/supplemental/10.1103/PhysRevB.88.081402 for additional TEM images showing iron-based particles encapsulated in MWCNTs.
[15]http://www.synchrotron-soleil.fr/portal/page/portal/Recherche/LignesLumiere/DIFFABS (accessed April 9, 2013).
[16]http://www.edmund-buehler.de/english/index.pml (accessed April 9, 2013).
[17]V. Heresanu, C. Castro, J. Cambedouzou, M. Pinault, O. Stephan, C. Reynaud, M. Mayne-L'Hermite, and P. Launois, J. Phys. Chem. C **112**, 7371 (2008).
[18]C. Prados, P. Crespo, J. M. Gonzàlez, A. Hernando, J. F. Marco, R. Gancedo, N. Grobert, M. Terrones, R. M. Walton, and H. W. Kroto, Phys. Rev. B **65**, 113405 (2002).
[19]J. F. Marco, J. R. Gancedo, A. Hernando, P. Crespo, C. Prados, J. M. Gonzàlez, N. Grobert, M. Terrones, D. R. M. Walton, and H. W. Kroto, Hyperfine Interact. **139/140**, 535 (2002)
[20]J. Cambedouzou, V. Heresanu, C. Castro, M. Pinault, F. Datchi, M. Mezouar, M. Mayne-L'Hermite, N. Bendiab, and P. Launois, Eur. Phys. J. B **72**, 145 (2009).
[21]D. Reznik, C. H. Olk, D. A. Neumann, and J. R. D. Copley, Phys. Rev. B **52**, 116 (1995).
[22]J. B. Nelson and D. P. Riley, Proc. Phys. Soc. **57**, 477 (1945).
[23]S. Bandow, Jpn. J. Appl. Phys., Part 2 **36**, L1403 (1997).
[24]Y. Maniwa, R. Fujiwara, H. Kira, H. Tou, E. Nishibori, M. Takata, M. Sakata, A. Fujiwara, X. Zhao, S. Iijima, and Y. Ando, Phys. Rev. B **64**, 073105 (2001).
[25]D. E. Gray, *American Institute of Physics Handbook*, 2nd ed. (McGraw-Hill, New York, 1963).
[26]P. Gorria, D. Martínez-Blanco, J. A. Blanco, M. J. Pérez, A. Hernando, L. Fernandez Barquín, and R. I. Smith, Phys. Rev. B **72**, 014401 (2005).
[27]J. A. Rodríguez-Manzo, M. Terrones, H. Terrones, H. W. Kroto, L. Sun, and F. Banhart, Nat. Nanotechnol. **2**, 307 (2007).
[28]M. Onink, C. M. Brakman, F. D. Tichelaar, E. J. Mittemeijer, S. van der Swaag, J. H. Root, and N. B. Konyer, Scr. Metall. Mater. **29**, 1011 (1993).
[29]B. Wei, M. Shima, R. Pati, S. K. Nayak, D. J. Singh, R. Ma, Y. Li, Y. Bando, S. Nasu, and P. M. Ajayan, Small **2**, 804 (2006).